Article

Scale Issue for Organic and Inorganic Carbon Exports to Oceans: Case Study in the Sub-Tropical Thukela River Basin, South Africa

Macdex Mutema [1], Sandiswa Figlan [2] and Vincent Chaplot [3,4,*]

1 Agricultural Research Council-Agricultural Engineering, Private Bag X519, Silverton, Pretoria 0127, South Africa
2 Department of Agriculture and Animal Health, University of South Africa, Private Bag X6, Florida 1710, South Africa
3 Laboratoire d'Océanographie et du Climat, Expérimentations et Approches Numériques, Institut de Recherche pour le Développement (IRD), UMR 7159, IRD-CNRS-UPMC-MNHN, 4 Place Jussieu, CEDEX 05, 75252 Paris, France
4 School of Agricultural, Earth and Environmental Sciences, University of KwaZulu-Natal, Private Bag X01, Scottsville, Pietermaritzburg 3209, South Africa
* Correspondence: vincent.chaplot@ird.fr

Abstract: Despite carbon (C) exports from continents being crucial in the connection between terrestrial, atmospheric, and oceanic C, there is still limited understanding of the dynamics of C within river basins. The objective of this work was to assess the changes in particulate (POC) and dissolved organic (DOC) and inorganic C (PIC: particulate inorganic carbon, DIC: dissolved inorganic carbon) content, quality, and fluxes within a river basin from its headwaters to its exit at the ocean. A survey was designed in the Thukela basin (from 2012 to 2013 and at six nested catchments ranging from ~10 to ~30,000 km^2) in the east of South Africa to evaluate the content, fluxes, and quality (UV spectral slope, ^{13}C, CO_2 effluxes from runoff) of the transported C in conjunction with chemical elements (Si, Na) for discriminating between the water sources and estimating C dynamics during low flows. Total carbon exports decreased continuously from 9.75 km^2 in the headwater (31.9 kg C km^{-2} y^{-1}) to ocean (4.7 kg C km^{-2} y^{-1}) with the highest decrease occurring between the catchment (7614 km^2) and large catchment (14,478 km^2). About 80% of C exports from the headwaters were POC, followed by DIC (10%) and DOC (10%), while at the ocean, the proportions were 31% (POC), 45% (DIC), 23% (DOC), and 0.7% (PIC). Moreover, there was a sharp decrease in the dissolved organic matter aromaticity from the headwater to ocean and for both DOC and POC that did not correspond to changes in water sources along the river (as indicated by a relatively constant Si/Na ratio). This pointed to the decomposition in the river of the dissolved organic matter originating from soils and to the within-stream organic production. Further in situ investigations need to be performed to quantify the within-stream inputs.

Keywords: organic compounds; river; chemistry; Africa; landscapes

1. Introduction

River basins export enormous amounts of carbon (C) from landscapes to the ocean (0.8–1.3 Pg C yr^{-1}, which is about 10% of the total annual C-CO_2 emissions due to fossil fuel combustion) and thus constitute a key element of the global C cycle. Their role in connecting the terrestrial, atmospheric, and oceanic C pools make them key in regulating the climate, soil, and water quality as well as a series of ecological functions. Previous studies have shown that C exports to the ocean are mostly in inorganic forms (60%) [1]. Organic exports amount to 0.22 and 0.18 Pg C yr^{-1} (40%) for dissolved (DOC) and particulate organic carbon (POC), respectively. Such exports constitute, however, a tiny fraction of the total

amount of C transported by rivers, reported as 8.4 and 1.3 Pg C yr^{-1} for DOC [2] and POC [3], respectively.

While rivers transport large amounts of organic C [4], the origin of the C reaching the ocean is still a matter of debate. Historically, exported DOC was thought to be old and recalcitrant, and transported conservatively from the headwaters to the ocean [5–8]. However, several recent studies have pointed to relatively "young C" exports dominated by within-stream produced DOC (e.g., [8–11]). Mayorga et al. [10] showed, for instance, that the DOC exported by the Amazon is less than 5 years old, while its headwaters transport comparatively old DOC, hundreds to thousands of years old. DOM undergoes a variety of biogeochemical reactions during downslope and downstream transportation to the ocean, which require further appraisal. Similarly, a considerable amount of river POM is lost during transit from upland soils in headwaters to rivers and the ocean due to several physical and chemical processes such as sedimentation, decomposition, humification, flocculation, and adsorption [12]. Meanwhile, POC transported by rivers is also degraded by micro- and macroinvertebrates, leading to the production of new and easily decomposable DOM [13].

There is not only a need to better understand the fluxes of DOM and POM in river basins from headwaters to the ocean, but also their quality as a means for a better understanding of the sources and dynamics of riverine OM. Properties of DOM and POM such as optical properties (absorbance and fluorescence), C content, C:N ratios, stable (δ^{13}C, δ^{15}N), radiocarbon isotopes (Δ^{14}C), and molecular properties can be used to quantify the changes in surface water OM as proxies of their dynamics. Several studies such as by Spencer et al. [14] have estimated the molecular weight of DOM using UV-absorbance to discriminate between allochthonous and autochthonous origin. In pursuit of a better understanding of the C dynamics in river basins, a study was implemented in Thukela basin, South Africa. Previous studies such as by Andersson et al. [15] and Mutema et al. [16] have published data on the yearly fluxes of runoff, sediment, and organic carbon within the Thukela River. Their results showed a general decrease in the fluxes in the downstream direction. Here, we aimed at complementing these research studies with data on the quality of the water and on the transported organic carbon, and due to the cost of the analyses, focusing on the headwaters to the ocean on low flows that constitute the main source of drinking water.

2. Materials and Methods

2.1. Study Site

Thukela is the largest river basin in the KwaZulu-Natal Province of South Africa, covering approximately 29,000 km^2 (Figure 1). The main river flows 502 km from the Drakensburg Mountains on the western side of the province to the Indian Ocean. The mean annual precipitation ranges from 550 mm yr^{-1} in the center of the basin to 2000 mm yr^{-1} in the steep slopes of the western area [15]. The basin climate is semi-arid with a mean annual rainfall and temperature of 588 mm and 27 °C, respectively. The main rain season starts around October and ends in April. The major land uses are subsistence farming and commercial forestry. The headwaters of the basin used in the current study are in a catchment known as Potshini, which is located at the foothills of the Drakensburg Mountains (29.37° E, 28.81° S and average altitude of 1310 m) and 10 km west of the town of Bergville. Its climate is classified as sub-tropical, with the long-term annual rainfall, temperature, and potential evaporation of 684 mm, 13 °C, and 1600 mm, respectively [17]. The rainy season is from September to April and is often characterized by thunderstorms and occasional hailstorms. Severe cold spells are sometimes experienced during winters (May to August). The geological formation underlying the Potshini catchment comprises sandstones, mudstones, and shale. A Karoo Dolerite dyke in the upper reaches of the catchment gives it specific weathering features such as rounded boulders.
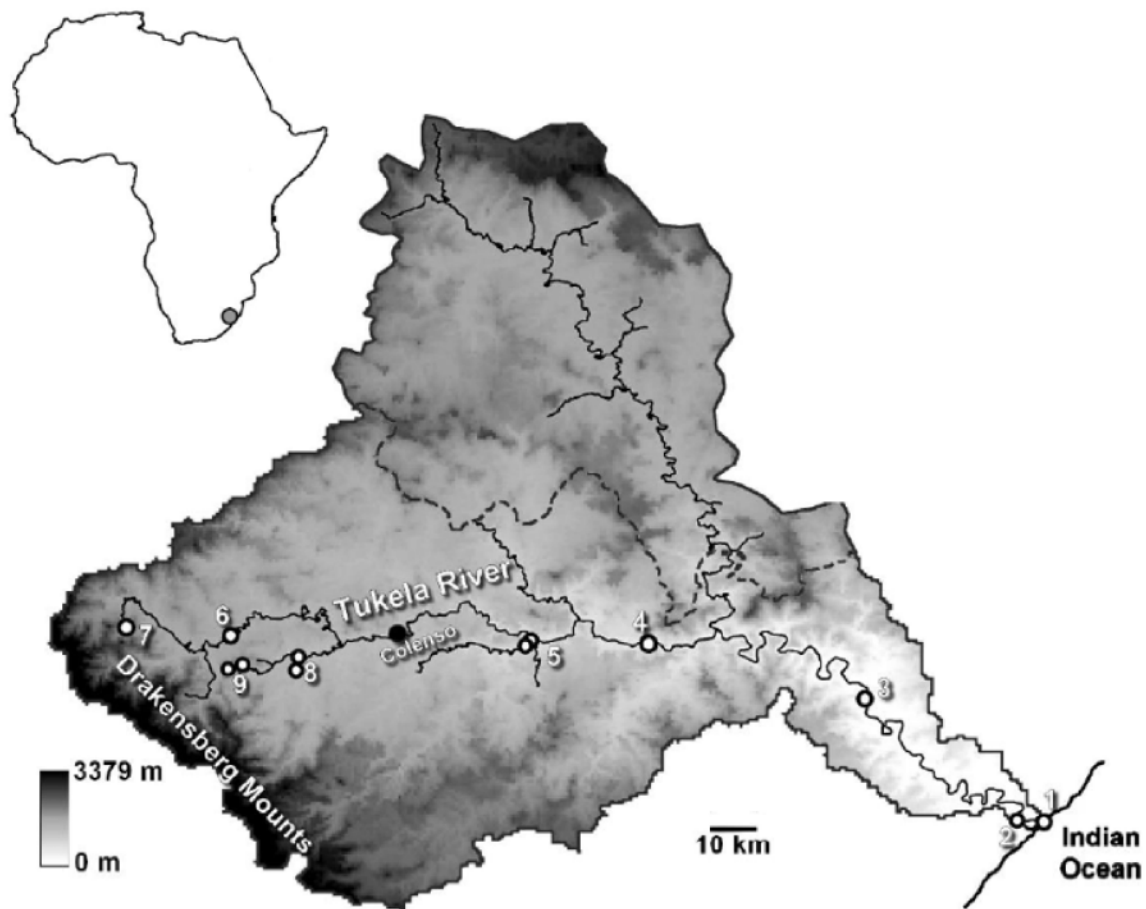
Figure 1. Locations of the Thukela basin in South Africa and the sampling data points.

2.2. Experimental Setup

The setup consisted of nested scales: a sub-catchment with a size of 9.7 km^2 (0.03% of the total river basin area; data point number 9, Figure 1), a 7614 km^2 catchment (26%; 5), followed by a 14,478 km^2 large catchment (50%; 4), a 27,845 km^2 sub-basin (96%; 3), and a 28,937 km^2 basin (100%; 2). The sub-catchment (9.75 km^2) to large catchment (14,478 km^2) outlets were equipped with differential pressure transducers for continuous monitoring of the stream stage (5-min intervals) and automatic samplers (ISCO Model 2900). The samplers were calibrated to sample more frequently during high flows (5-min intervals) and less during low flows where sampling only occurred once a week. Sampling events were captured by dataloggers (CR200), making it possible to know precisely when each sample was collected. Flow at the sub-catchment outlet was also monitored every 5 min by a pressure transducer at a road culvert. Another culvert near Winterton (29.10° E, 28.79° S) with similar equipment and sampling strategy was used at the sub-basin outlet. Daily flow data for the basin outlet at Mandeni (31.39° E, 29.14° S) was obtained from the Department of Water Affairs and Forestry, Republic of South Africa.

2.3. Sampling Procedure

Complementary to previous studies that investigated water, sediment, and carbon fluxes for entire years [15,16], the field sampling for the dissolved and particulate organic and inorganic carbon, and the water quality and fluxes was carried out on the four dates during low flow periods in 2012 (12 June, 2 November) and in 2013 (25 March; 15 October). Equipment at the catchment outlets measured and stored the flow data, which were used to compute the surface runoff (R, L day^{-1} km^{-2}). Grab samples were collected at all sampling dates and surface areas for the estimation of sediment concentration (SC) as well as for the POC, PON, and PIC contents and water quality. The one-liter water samples were

immediately filtered through 0.45 µm filters for the DIC and DOC estimations. The filters were dried at 25 °C and the sediments analyzed for SC, PIC, and POM estimation. The filtered water samples were preserved by adding two drops of 2 N HCl (pH 2) for further evaluation in the laboratory. All water samples were stored in the dark at 4 °C for further estimation of the DOC, DIC concentration, and quality.

2.4. Characterization of DOM and POM

Sediment samples were analyzed for the total particulate organic C content (POC_C) using a dry matter combustion method using the LECO CNS–2000 Dumas analyzer (LECO corp., St. Joseph, MI, USA). Total dissolved (<0.45 µm) organic C in the water samples (DOC_C) was estimated using a Shimadzu TOC-5000 analyzer with an ASI-5000 autosampler and a Balston 78–30 high purity gas generator (Shimadzu, Tokyo, Japan). The DOM quality was assessed using a UVmini-1240 UV–VIS spectrophotometer (Spencer et al., 2010; Krupa et al., 2011). A single quartz cuvette (0.01 m, rinsed three times) was used to measure the absorbance spectra of the filtered water samples. Therefore, the DOC data used in the current analysis were the averages of 3 replicate injections for which the coefficient of variance was always less than 1%. The aromaticity and molecular weight of DOM are correlated to UV absorbance [18]. Spectral slopes between 275 and 295 nm ($S_{275-295}$) and 290–350 nm ($S_{290-350}$) were considered by the current study because they allow for a variety of DOM compounds to be discriminated [19]. Nevertheless, the DOM quality was subsequently accessed using direct measurements of CO_2 effluxes from the filtered water samples with the assumption that DOM decomposition dynamics correlate with the DOM quality. The CO_2 assessments were performed on 200 mL aliquots of the filtered water samples incubated in 1000 mL open-top jars for 7 days in a 100% humidity environment at 20 ± 2 °C [20]. The CO_2 emissions were assessed daily using an LI-6400XT portable photo-synthesis analyzer (Li-Cor Inc., Lincoln, NE, USA). The measurements were taken at 2 min intervals per sample (taking three measurements in ppm). Constant headspace was maintained in each jar throughout the experiment by closing the jars after measurement to limit the water loss to evaporation. The jars were opened daily for 30 min prior to the CO_2 efflux measurements (to allow for equilibrium before measurements) and were left open throughout the experiment to avoid errors that rise from disturbances of the equilibrium between the atmosphere and system. Samples were checked for change in mass by weighing the jars every day after each gas sampling (to monitor the possible changes in headspace).

3. Results

3.1. Variability in Runoff and Chemical Elements

The results in Table 1 showed a continuous decrease in runoff in the downstream direction from the sub-catchment (904 ± 180 L day^{-1} km^{-2}) to large catchment (164 ± 12 L day^{-1} km^{-2}), followed by an increase in the sub-basin to basin (192 ± 7 L day^{-1} km^{-2}) scale. The change in the spatial scale also impacted the chemical elements assessed (Table 1). The concentrations of Si, Zn, Ca, and HCO_3 increased through the different catchment sizes to reach the maximum values at the basin level. For instance, Si rose from 57.5 ± 8.6 mg L^{-1} at the sub-catchment to 71.3 ± 5.7 mg L^{-1} at the large catchment and to 85.2 ± 4.3 mg L^{-1} at the basin level (Table 1), which corresponded to an increase from the spring to outlet of about 50%. Na and Fe showed a different behavior, with values first increasing to the catchment level, then decreasing to the large catchment, to subsequently decreasing to the sub-basin before sharply increasing (values more than doubled in case of Fe) to the basin outlet. Mn stagnated between the catchment and large catchment scale, then declined at the sub-basin scale before increasing sharply at the basin scale. Mg and K increased from the catchment to large catchment scale. However, their trends differed thereafter, with Mg increasing to the sub-basin scale and then decreasing at the basin scale. The basin scale Mg concentration was still greater than at all the other catchment scales, except for the sub-basin. On the other hand, K decreased at the sub-basin scale, followed by a 2-fold increase at the basin scale. In all cases, the standard errors, which were computed from the

different sampling dates, were below 20%. There was, however, a tendency for the standards errors (i.e., the differences between the sampling dates) to be the highest in the headwater and the lowest at the basin outlet.

Table 1. The mean values of distance from the river outlet (D), surface area (A, percentage of the total basin surface area in italic), runoff (R, L day^{-1} km^{-2}) from low flows, and the content $\pm$ standard error of the mean in chemical elements at each sampling site (with numbers extracted from Figure 1).

Sampling Site	A (A%)	D	R	SC	Si	Na	Mn	Fe	Zn	Ca	Mg	K	HCO$_3$
	km^2	km	L day^{-1} km^{-2}	g L^{-1}	mg L^{-1}								
Sub catchment (9)	9.75 (0.03%)	433.8	904 $\pm$ 180	0.14 $\pm$ 0.03	57.5 $\pm$ 8.6	1.6 $\pm$ 0.2	25.0 $\pm$ 4.0	365 $\pm$ 58	7.5 $\pm$ 1.2	5.5 $\pm$ 0.9	2.3 $\pm$ 0.4	0.8 $\pm$ 0.1	48.5 $\pm$ 5.8
Catchment (5)	7614 (26%)	275.6	301 $\pm$ 62	0.08 $\pm$ 0.01	68.5 $\pm$ 6.9	2.5 $\pm$ 0.2	28.3 $\pm$ 3.0	633 $\pm$ 67	12.9 $\pm$ 1.4	10.5 $\pm$ 1.2	5.1 $\pm$ 0.6	1.9 $\pm$ 0.2	58.2 $\pm$ 4.6
Large catchment (4)	14,478 (50%)	230.6	164 $\pm$ 12	0.02 $\pm$ 0.00	71.3 $\pm$ 5.7	1.8 $\pm$ 0.1	28.3 $\pm$ 2.4	305 $\pm$ 26	16.5 $\pm$ 1.4	17.5 $\pm$ 1.6	9.6 $\pm$ 0.9	3.7 $\pm$ 0.4	114.5 $\pm$ 7.3
Sub-basin (3)	27,845 (96%)	7.1	191 $\pm$ 8	0.02 $\pm$ 0.00	78.3 $\pm$ 3.9	2.3 $\pm$ 0.1	23.2 $\pm$ 1.2	413 $\pm$ 22	23.7 $\pm$ 1.3	21.2 $\pm$ 1.2	12.0 $\pm$ 0.7	2.9 $\pm$ 0.2	120.4 $\pm$ 4.8
Basin (2)	28,937 (100%)	0	192 $\pm$ 7	0.01 $\pm$ 0.00	85.2 $\pm$ 4.3	3.6 $\pm$ 0.2	29.7 $\pm$ 1.6	971 $\pm$ 52	34.0 $\pm$ 1.9	22.0 $\pm$ 1.2	10.0 $\pm$ 0.6	5.3 $\pm$ 0.3	155.6 $\pm$ 6.2

3.2. Variations in C Concentrations in Runoff and Sediments

The POC, PIC, DOC, and DIC contents highly varied from the headwater to ocean (Table 2). POCc and PICc exhibited a general increase from the sub-catchment to sub-basin, followed by a decrease at the basin outlet (Table 2). For instance, POCc in the transported sediments rose from 0.55 $\pm$ 0.12% at the sub-catchment level to 3.74 $\pm$ 0.18% at the sub-basin, which corresponded to a 6.8-fold increase that was significant at the $p < 0.05$ level. The subsequent decrease in POCc was 44%. There was no inorganic carbon in the headwater sediments but PICc rose to 0.27 $\pm$ 0.01% at the sub-basin level to thereafter decrease to 0.05 $\pm$ 0.002% (Table 2). With about 10 mg L^{-1}, the DOCc and DICc were almost identical at the sub-catchment level, but the trend was for DICc to continuously rise to the ocean (to 30.63 $\pm$ 1.63 mg C L^{-1}), while for POCc, DOCc only increased to the sub-basin (21.91 $\pm$ 1.17 mg C L^{-1}) to subsequently decrease to the ocean (15.59 $\pm$ 0.83 mg C L^{-1}).

Table 2. Mean values of the particulate organic carbon content (POCc), particulate nitrogen content (PONc), dissolved organic carbon content (DOCc), particulate inorganic carbon content (PICc), dissolved inorganic carbon content (DICc), ratio between POCc and PONc (C/N), isotopic concentration of ^{13}C in POC (^{13}C), cumulative CO$_2$ emissions from sediments over 120 days (CO$_2$), spectral slopes between 275 and 295 nm ($S_{275-295}$), and the spectral slope ratio between $S_{275-295}$ and $S_{290-350}$ (S_R) $\pm$ standard error of the mean at each sampling site.

Sampling Site	POCc	PONc	PICc	DOCc	DICc	C/N	^{13}C	CO$_2$	$S_{275-295}$	S_R
	%			mg L^{-1}			‰	mgC-CO$_2$ m^{-2}	Nm^{-1}	
Sub catchment (9)	0.55 $\pm$ 0.12	0.09 $\pm$ 0.01	0.00 $\pm$ 0.00	9.68 $\pm$ 1.55	9.91 $\pm$ 1.59	6.33 $\pm$ 1.04$\pm$	-20.31 ± 3.45	1.21 $\pm$ 0.21	10.90 $\pm$ 1.96	1.06 $\pm$ 0.13
Catchment (5)	1.36 $\pm$ 0.24	0.84 $\pm$ 0.08	0.00 $\pm$ 0.00	17.43 $\pm$ 2.86	11.84 $\pm$ 1.26	4.46 $\pm$ 0.49	-19.63 ± 2.22	1.29 $\pm$ 0.15	12.53 $\pm$ 1.50	1.20 $\pm$ 0.10
Large catchment (4)	1.66 $\pm$ 0.19	0.23 $\pm$ 0.02	0.12 $\pm$ 0.01	20.00 $\pm$ 1.71	24.21 $\pm$ 2.07	7.40 $\pm$ 0.65	-17.53 ± 1.59	0.97 $\pm$ 0.09	8.29 $\pm$ 0.79	1.28 $\pm$ 0.08
Sub-basin (3)	3.74 $\pm$ 0.18	0.64 $\pm$ 0.03	0.27 $\pm$ 0.01	21.91 $\pm$ 1.17	32.70 $\pm$ 1.74	5.79 $\pm$ 0.32	-21.89 ± 1.24	1.29 $\pm$ 0.07	5.77 $\pm$ 0.30	1.30 $\pm$ 0.05
Basin (2)	2.10 $\pm$ 0.08	0.34 $\pm$ 0.00	0.05 $\pm$ 0.00	15.59 $\pm$ 0.83	30.63 $\pm$ 1.63	6.26 $\pm$ 0.34	-20.58 ± 1.10	1.21 $\pm$ 0.07	6.52 $\pm$ 0.39	1.29 $\pm$ 0.05

PONc showed a different trend than both the organic and inorganic C as it rose from the sub-catchment to catchment, decreased to the large catchment, and increased to the sub-basin before subsequently decreasing to the basin level. The C/N ratio behaved in contrast to PONc: a decrease from the sub-catchment to catchment, an increase to the large-catchment, a decrease to the sub-basin, and an increase to basin (Table 2). The content of ^{13}C in POC as CO$_2$ effluxes from the runoff increased from the sub-catchment to large catchment, and for DOCc, it increased to the sub-basin to decrease to the basin level. $S_{275-295}$, which depicts the quality of dissolved organic matter, showed a general decrease to the sub-basin, followed by an increase to the ocean.

3.3. Spatial Scale Issue on Organic and Inorganic C Fluxes

The total C exports (CL) (i.e., the sum of particulate and dissolved organic and inorganic C) decreased continuously from the headwaters where it reached a maximum of 87.4 $\pm$ 14.0 g C day^{-1} km^{-2} to the ocean where it decreased to 12.9 $\pm$ 0.25 g C day^{-1} km^{-2}

(Table 3). This corresponded to a 6.7 time decrease, significant at the 0.05 level. CL decreased from the sub-catchment to catchment by half, and by a factor of 3 to the large catchment level. The decrease in CL to the ocean corresponded to a decrease in POC losses and in the POC contribution to CL. Indeed, on one hand, the POCL decreased from 69.6 ± 15.3 g C day^{-1} km^2 at the sub-catchment outlet to 4.0 ± 0.06 g C day^{-2} at the basin outlet, which corresponded to a 17.3 decrease (Table 3). On the other hand, 80% of C exports from the headwaters were POC followed by DIC (10%) and DOC (10%), while at the ocean, the proportions of POC decreased to 31% for POC, 45% (DIC), 23% (DOC), and 0.7% (PIC).

Table 3. The mean values of the particulate organic C losses (POCL), particulate inorganic C losses (PICL), dissolved organic C losses (DOCL), and dissolved inorganic C losses (DICL) expressed for each surface area in kg of C and in percent of the total carbon losses (CL) $\pm$ standard error of the mean at each sampling site.

Sampling Site	POCL	PICL	DOCL	DICL	CL	POCL	PICL	DOCL	DICL
	g C day^{-1} km^{-2}					%			
Sub catchment (9)	69.6 ± 15.3	0.00 ± 0.00	8.96 ± 1.26	8.7 ± 1.4	87.4 ± 14.0	79.7 ± 13.2	0.00 ± 0.00	10.0 ± 1.8	10.3 ± 1.9
Catchment (5)	32.8 ± 5.9	0.00 ± 0.00	3.56 ± 0.33	5.3 ± 0.5	41.6 ± 4.4	78.8 ± 8.0	0.00 ± 0.00	12.6 ± 1.5	8.6 ± 1.0
Large catchment (4)	5.5 ± 0.5	0.38 ± 0.03	3.97 ± 0.27	3.3 ± 0.3	13.2 ± 1.1	41.6 ± 3.6	3.00 ± 0.27	25.1 ± 2.3	30.3 ± 2.0
Sub-basin (3)	14.4 ± 0.7	1.04 ± 0.03	6.27 ± 0.27	4.2 ± 0.2	25.8 ± 1.4	55.5 ± 3.1	4.00 ± 0.22	16.3 ± 1.0	24.3 ± 1.5
Basin (2)	4.0 ± 0.1	0.11 ± 0.00	5.86 ± 0.10	3.0 ± 0.1	12.9 ± 0.3	31.0 ± 1.7	0.70 ± 0.04	23.0 ± 1.3	45.2 ± 2.7

3.4. Factors Controlling POM and DOM Fluxes and Quality

The correlation indices (r) represent the one-on-one relationships between the variables of organic matter quality such as ^{13}C, CO_2, C/N, and the spectral characteristics of dissolved organic matter on one hand, and the surface area, runoff, and content of chemical elements on the other hand. ^{13}C was significantly negatively correlated with A, Si, Na, Ca, and HCO_3 with correlation coefficients varying between -0.65 and -0.82. Nevertheless, the same factors (A, Si, Na, Ca and HCO_3) correlated positively with S_R, with superior correlation coefficients (r = 0.86–0.96) than ^{13}C, except for Na (r = 0.57). While A also showed a strongly negative correlation with $S_{275-295}$ (r = -0.91), R correlated negatively with CO_2 (r = -0.96) but positively with C/N ratio (r = 0.93). Amongst the carbon content variables, only DICc showed a significant correlation with the "quality" variables, but only with S275–295 (r = 0.97). In contrast, Na correlated positively with CO_2 (r = 0.59) and negatively with the C/N ratio (-0.50). However, the correlations were weaker in comparison to both A and R. Ca (r = -0.90) and HCO_3 (r = -0.94) exhibited strongly negative correlations with $S_{275-295}$, while PONc correlated positively with the C/N ratio (r = 0.83).

A PCA, showing the multiple-relationships between the variables under study and surface area (A), displayed as a secondary variable (i.e., a variable not used for axis construction), is presented in Figure 2. The two major axes of the PCA accounted for 77% of the dataset variability with PC1 accounting for 43%, while PC2 accounted for 34%. PC1 exhibited a strong relationship with S_R with positive coordinates and POCc; $Sr_{275-295}$ and DOCc and DICc with negative coordinates. PC2, on the other hand, was associated with R and C/N with positive coordinates, and CO_2 with negative coordinates. Therefore, PC1 could thus be interpreted as an axis of C content and aromaticity, while PC2 could be interpreted as an axis of water and CO_2 fluxes. In this PCA, the C content (POCc, DOCc, and DICc) tended to increase with surficial area of the catchment scale. Additionally, as the C content increased, the POM and DOM aromaticity tended to decrease as depicted by high $Sr_{275-295}$, ^{13}C content, and S_R values (e.g., [21]). Surprisingly, water fluxes and CO_2 from the runoff did not correlate with the surface area.
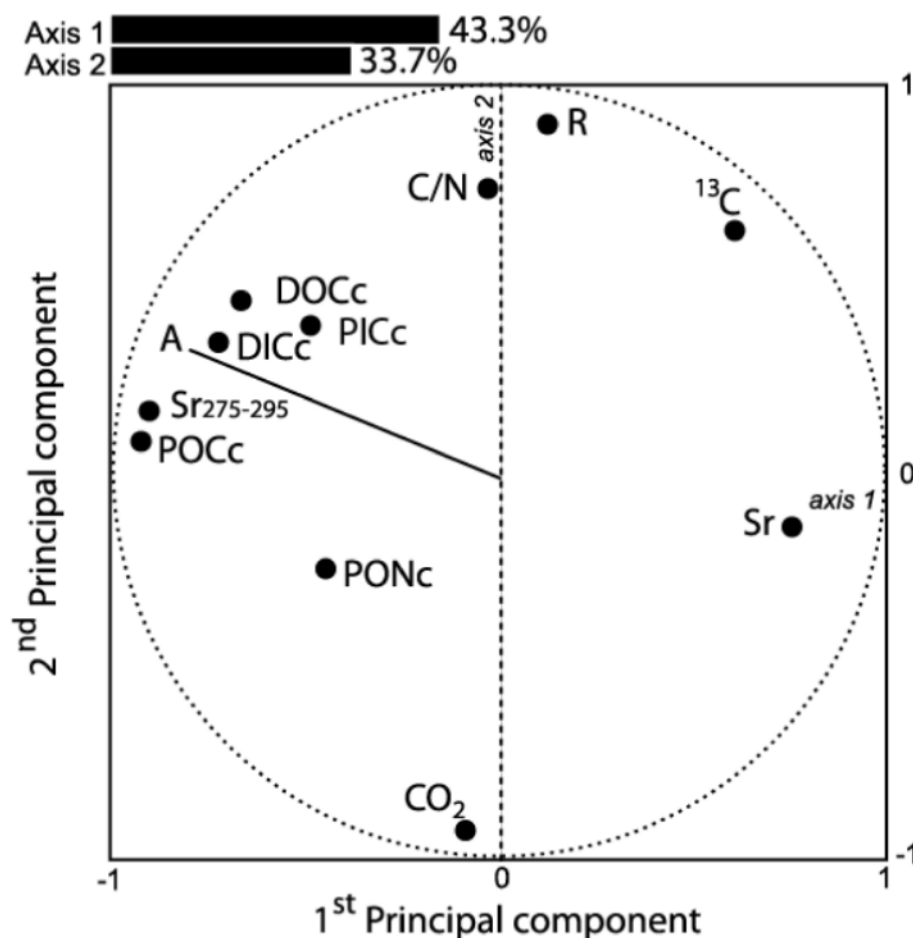
Figure 2. Principal component analysis of the variables under study: distance from the river outlet (D), surface area (A), runoff (R), particulate organic carbon content (POCc), particulate nitrogen content (PONc), dissolved organic carbon content (DOCc), particulate inorganic carbon content (PICc), dissolved inorganic carbon content (DICc), ratio between POCc and PONc (C/N), isotopic concentration of ^{13}C in POC (^{13}C), cumulative CO_2 emissions from sediments over 120 days (CO_2), spectral slopes between 275 and 295 nm ($S_{275–295}$), and spectral slope ratio between $S_{275–295}$ and $S_{290–350}$ (S_R). All variables were used for PCA construction except A, the surface area, which was only used as a display.

4. Discussion

4.1. On the Fluxes and Sources of Water from Headwater to the Ocean

The results of the current pointed to a decrease in the unit-area runoff (i.e., liters of runoff per day and per km^2) with an increasing basin surface area (A) to 50% of the total area of the Thukela River basin, followed by an increase to the ocean. Such a decrease in R with increasing A has been widely reported in many studies (e.g., [22–25]); following the meta-analysis by Mutema et al. [26], this is common in dry climates. This trend can be attributed to riverbed infiltration, and another possible explanation in the area is water uptake for agriculture and drinking water. The subsequent R increase to the ocean could be due to the exfiltration of the initially infiltrated rainwater. Water input from overland flow could be negligible because the assessments were performed during low flow periods. Indeed, large amounts of overland flow infiltrate during the downslope to downstream course of overland flow in non-channelized flow systems due to the presence of physical barriers to surface flow such as furrows or tree lines and grass strips [27,28]. The infiltrated water could reach the water table before gradually exfiltrating in the downstream direction, thus explaining the increase in the unit-area runoff. The presence of Na in the runoff water samples confirmed a hypothesis of groundwater contribution to runoff of up to at least

50% of the Thukela River basin area. The decrease in R beyond 50% of the total basin surface area could be, as indicated above, due to riverbed infiltration, evaporation from water bodies, and water uptake by human activities such as the irrigation of croplands and uptake by cities and industries, as observed within the Thukela River basin.

4.2. On the Link between Runoff and POM and DOM Content and Quality

The higher POCc and PONc in the runoff at the basin outlet than in the headwaters was surprising because many studies have observed higher values at the hillslope level compared to the basin outlet (e.g., [29,30]). The authors generally explained such a decrease by the decrease in unit-area runoff and the associated transport capacity of POC and PON [26,31,32]. The fact that the runoff and sediment concentration in the runoff decreased to the ocean is indicative of the decreasing capacity of runoff to transport soil material. The increase in carbon transport from the headwater to the ocean could not thus be explained by an increasing transport capacity. Another possible explanation for the increasing POC and PON contents is the production in the stream of easy to transport organic material, which needs further appraisal. The increase in the PIC content in the lower basin where sugar cane is present might be due to anthropic activities such as liming and/or outputs from rocks [33].

The DOCc observed in the current study, varying between 9.7 and 21.9 mg C L^{-1}, was relatively higher than from the river basins reported in the available literature (e.g., [34–37]). Coynel et al. [34] reported lower values for the Ubangi River in Congo, as did Hammand et al. [35] for the Essequibo River in Guyana (5.0 mg C L^{-1}), Spencer et al. [36] for the Mobile River (5.5 mg C L^{-1}), Hudson (5.3 mg C L^{-1}) and Afchafalaya Rivers (5.2 mg C L^{-1}) in the U.S.; and Spencer et al. [37] for the Kolyma in Siberia (5.5 mg C L^{-1}). However, these values are not too far off from the findings of Mutema et al. [16] for the same river basin (1.31–20.44 mg C L^{-1}; with a mean of 5.13 mg C L^{-1}). However, it is important to note that the results from Mutema et al. (2017) were based on a longer duration covering both high and low flows. The high DOCc recorded in the current study may also be explained by the fact that the low flow sampling ensured that there was no rainwater dilution effect compared to high flows [38].

The increase in the organic C content during the downstream course of water is generally attributed to either the within-stream production or lateral input [39,40]. The fact that DOCc increased with the unit-area surface runoff in the current study has already been alluded to. This increase in DOCc in the downstream direction also coincided with decreasing S$_{275–295}$ values, which depicts an improving dissolved organic matter quality [36]. The decrease in the S$_{275–295}$ values is associated with a reduction in dissolved organic matter of higher molecular weight and greater aromaticity such as humic acids from soils [21]. The notion of the decreasing content of dissolved organic matter of high molecular weight and aromaticity appear to be supported by the general increase in S$_R$ values in the downstream direction (Table 2). Thus, the increase in DOCc in the current study is most likely to be due to inputs of "relatively young" organic matter, which is more likely to emanate from within-stream production than lateral inputs from soils where the organic matter is of high aromaticity. The increase in DOCc was also associated with increasing DICc in the downstream direction. The average value of DICc at the basin outlet (31 mg C L^{-1}) was consistent was higher than the 20 mg C L^{-1} reported for temperate climate basins, but very significantly higher than the 6 mg C L^{-1} reported for tropical basins [26]. This sharp increase in DICc from the headwaters to the ocean observed in a river basin dominated by subsistence farming and commercial forestry requires further investigation. Amongst the possible explanations, Wen et al. [1] indicated that during low flows (which corresponds to the conditions of the present study), longer water transits led to the mineralization of organic carbon into inorganic carbon, thus potentially explaining the increase in inorganic C content in the downstream direction. Such a mechanism has been demonstrated to be the most efficient in large river networks from the tropics than in temperate and Arctic regions in cold watersheds [8].

5. Conclusions

The main objective of this study was to evaluate the organic and inorganic carbon (C) fluxes at different spatial scales in order to better understand the C dynamics in a sub-tropical river basin. While the total C losses decreased by 6-fold from the headwaters to ocean, it can be concluded that exports from the headwaters were 90% for organics vs. 10% for inorganics, and exports to the ocean were 54% organic vs. 46% inorganic. At the same time, exports from the headwaters were 79.7% particulate vs. 20.3% dissolved while at the basin outlet, C exports were 68.2% dissolved vs. 31.7% particulate. The second conclusion that was drawn from the quality of the organic compounds was the existence of dissolved inorganic and organic inputs during the downstream course of runoff, resulting or not from within-stream production. Further research focusing on the sources of dissolved C is needed.

Author Contributions: V.C. conceptualysed the research, M.M. and S.F. gather data, analyse them and write the first draft of the paper that was improved his two co-authors. All authors have read and agreed to the published version of the manuscript.

Institutional Review Board Statement: Not applicable.

Informed Consent Statement: The participation of the three authors was completely voluntary.

Data Availability Statement: The authors make all data available.

Conflicts of Interest: The authors declare no conflict of interest.

References

1. Wen, H.; Sullivan, P.L.; Billings, S.A.; Ajami, H.; Cueva, A.; Flores, A.; Hirmas, D.R.; Koop, A.N.; Murenbeeld, K.; Zhang, X.; et al. From soils to streams: Connecting terrestrial carbon transformation, chemical weathering, and solute export across hydrological regimes. *Water Resour. Res.* **2022**, *58*, e2022WR032314. [CrossRef]
2. Chaplot, V.; Mutema, M. Sources and main controls of dissolved organic and inorganic carbon in river basins: A worldwide meta-analysis. *J. Hydrol.* **2021**, *603*, 126941. [CrossRef]
3. Müller-Nedebock, D.; Chaplot, V. Soil carbon losses by sheet erosion: A potentially critical contribution to the global carbon cycle. *Earth Surf. Process. Landf.* **2015**, *40*, 1803–1813. [CrossRef]
4. Schlesinger, W.H.; Melack, J.M. Transport of organic carbon in the world's rivers. *Tellus* **1981**, *33*, 172–187.
5. Bianchi, T.S.; Filley, T.; Dria, K.; Hatcher, P.G. Temporal variability in sources of dissolved organic carbon in the lower Mississippi river. Geochim. Cosmochim. *Acta* **2004**, *68*, 959–967.
6. Martoura, R.F.C.; Woodward, E.M.S. Conservative behavior of riverine dissolved organic carbon in the Severn estuary: Chemical and geochemical implications. *Geochim. Cosmochim. Acta* **1983**, *47*, 1293–1309. [CrossRef]
7. Van Heemst, J.D.; Megens, L.; Hatcher, P.G.; de Leeuw, J.W. Nature, origin and average age of estuarine ultrafiltered dissolved organic matter as determined by molecular and carbon isotope characterization. *Org. Geochem.* **2000**, *31*, 847–857. [CrossRef]
8. Liu, S.; Wang, P.; Huang, Q.; Yu, J.; Pozdniakov, S.P.; Kazak, E.S. Seasonal and spatial variations in riverine DOC exports in permafrost-dominated Arctic river basins. *J. Hydrol.* **2022**, *612*, 128060. [CrossRef]
9. Raymond, P.A.; Bauer, J.E. DOC cycling in a temperate estuary: A mass balance approach using natural 14C and 13C isotopes. *Limnol. Oceanogr.* **2001**, *46*, 655–667. [CrossRef]
10. Mayorga, E.; Aufdenkampe, A.K.; Masiello, C.A.; Krusche, A.V.; Hedges, J.I.; Quay, P.D.; Brown, T.A. Young organic matter as a source of carbon dioxide outgassing from Amazonian rivers. *Nature* **2005**, *436*, 538–541. [CrossRef]
11. Ishikawa, N.F.; Butman, D.; Raymond, P.A. Radiocarbon age of different photoreactive fractions of freshwater dissolved organic matter. *Org. Geochem.* **2019**, *135*, 11–15. [CrossRef]
12. Sharp, E.L.; Parsons, S.A.; Jefferson, B. Seasonal variations in natural organic matter and its impact on coagulation in water treatment. *Sci. Total Environ.* **2006**, *363*, 183–194. [CrossRef]
13. Monahan, E.C.; Dam, H.G. Bubbles: An estimate of their role in the global oceanic flux of carbon. *J. Geophys. Res. Ocean.* **2001**, *106*, 9377–9383. [CrossRef]
14. Spencer, R.G.; Aiken, G.R.; Wickland, K.P.; Striegl, R.G.; Hernes, P.J. Seasonal and spatial variability in dissolved organic matter quantity and composition from the Yukon River basin, Alaska. *Glob. Biogeochem. Cycles* **2008**, *22*. [CrossRef]

15. Andersson, J.C.M.; Zehnder, A.J.B.; Jewitt, G.P.W.; Yang, H. Water availability, demand and reliability of in situ water harvesting in smallholder rain-fed agriculture in the Thukela River Basin, South Africa. Hydrol. *Earth Syst. Sci.* **2009**, *13*, 2329–2347. [CrossRef]

16. Mutema, M.; Chivenge, P.; Nivet, F.; Rabouille, C.; Thieu, V.; Chaplot, V. Changes in carbon and nutrient fluxes from headwaters to ocean in a mountainous temperate to subtropical basin. *Earth Surf. Process. Landf.* **2017**, *42*, 2038. [CrossRef]

17. Schulze, R. *South African Atlas of Agro Hydrology and Climatology*; TT82/96; Water Research Commission, Republic of South Africa: Pretoria, South Africa, 1997.

18. Weishaar, J.L.; Aiken, G.R.; Bergamaschi, B.A.; Fram, M.S.; Fujii, R.; Mopper, K. Evaluation of specific ultraviolet absorbance as an indicator of the chemical composition and reactivity of dissolved organic carbon. *Environ. Sci. Technol.* **2003**, *37*, 4702–4708. [CrossRef]

19. Aiken, G.R.; Hsu-Kim, H.; Ryan, J.N. Influence of dissolved organic matter on the environmental fate of metals, nanoparticles and colloids. *Environ. Sci. Technol.* **2011**, *45*, 3196. [CrossRef]

20. Fang, C.; Moncrieff, J.B. The dependence of soil CO_2 efflux on temperature. *Soil Biol. Biochem.* **2001**, *33*, 155–165. [CrossRef]

21. Sickman, J.O.; DiGiorgio, C.L.; Davisson, M.L.; Lucero, D.M.; Bergamaschi, B. Identifying sources of dissolved organic carbon in agriculturally dominated rivers using radiocarbon age dating: Sacramento–San Joaquin River Basin, California. *Biogeochemistry* **2010**, *99*, 79–96. [CrossRef]

22. Van de Giesen, N.C.; Stomph, T.J.; de Ridder, N. Scale effect of Hortonian overland flow and rainfall-runoff dynamics in a West African catena landscape. *Hydrol. Process.* **2000**, *14*, 165–175. [CrossRef]

23. Joel, A.; Messing, I.; Seguel, O.; Casanova, M. Measurement of surface water runoff from plots of two different sizes. *Hydrol. Process.* **2002**, *16*, 1467–1478. [CrossRef]

24. Asadzadeh, F.; Gorji, M.; Vaezi, A.; Sokouti, R.; Shorafa, M. Scale effect on runoff from field plots under natural rainfall. *Am.-Eur. J. Agric. Environ. Sci.* **2012**, *12*, 1148–1152.

25. Thomaz, E.L.; Vestena, L.R. Measurement of runoff and soil loss from two differently sized plots in a subtropical environment (Brazil). *Earth Surf. Process. Landf.* **2012**, *37*, 363–373. [CrossRef]

26. Mutema, M.; Chaplot, V.; Jewitt, G.; Chivenge, P.; Blöschl, G. Annual water, sediment, nutrient, and organic carbon fluxes in river basins: A global meta-analysis as a function of scale. *Water Resour. Res.* **2015**, *51*, 8949–8972. [CrossRef]

27. Cammeraat, E.L.H. Scale dependent thresholds in hydrological and erosion response of a semi-arid catchment in southeast Spain. *Agric. Ecosyst. Environ.* **2004**, *104*, 317–332. [CrossRef]

28. Mayor, A.G.; Bautista, S.; Bellot, J. Scale-dependent variation in runoff and sediment yield in a semiarid Mediterranean catchment. *J. Hydrol.* **2011**, *397*, 128–135. [CrossRef]

29. Le Bissonnais, Y.; Benkhadra, H.; Chaplot, V.; Fox, D.; King, D.; Daroussin, J. Crusting, runoff and sheet erosion on silty loamy soils at various scales and upscaling from m2 to small catchments. *Soil Tillage Res.* **1998**, *46*, 69–80. [CrossRef]

30. Parsons, A.J.; Brazier, R.E.; Wainwright, J.; Powell, D.M. Scale relationships in hillslope runoff and erosion. *Earth Surf. Process. Landf.* **2006**, *31*, 1384–1393. [CrossRef]

31. Doble, R.; Brunner, P.; McCallum, J.; Cook, P.G. An analysis of riverbank slope and unsaturated flow effects on bank storage. *Groundwater* **2012**, *50*, 77–86. [CrossRef]

32. Eder, A.; Exner-Kittridge, M.; Strauss, P.; Blöschl, G. Re-suspension of bed sediment in a small stream–results from two flushing experiments. *Hydrol. Earth Syst. Sci.* **2014**, *18*, 1043–1052. [CrossRef]

33. Zhang, Y.; Jiang, Y.; Yuan, D.; Cui, J.; Li, Y.; Yang, J.; Cao, M. Source and flux of anthropogenically enhanced dissolved inorganic carbon: A comparative study of urban and forest karst catchments in Southwest China. *Sci. Total Environ.* **2020**, *725*, 138255. [CrossRef] [PubMed]

34. Coynel, A.; Seyler, P.; Etcheber, H.; Meybeck, M.; Orange, D. Spatial and seasonal dynamics of total suspended sediment and organic carbon species in the Congo River. Glob. Biogeochem. *Cycles* **2005**, *19*, GB4019. [CrossRef]

35. Hammond, E.G.; Johnson, L.A.; Su, C.; Wang, T.; White, P.J. Soybean oil. In *Bailey's Industrial Oil and Fat Products*, 6th ed.; John Wiley & Sons, Inc.: Hoboken, NJ, USA, 2005.

36. Spencer, R.G.M.; Butler, K.D.; Aiken, G.R. Dissolved organic carbon and chromophoric dissolved organic matter properties of rivers in the USA. *J. Geophys. Res.* **2012**, *117*, G03001. [CrossRef]

37. Drake, T.; Wickland, K.; Spencer, R.; Striegl, R. Ancient low–molecular-weight organic acids in permafrost fuel rapid carbon dioxide production upon thaw. *Proc. Natl. Acad. Sci. USA* **2015**, *112*, 13946–13951. [CrossRef] [PubMed]

38. Chaplot, V.; Ribolzi, O. Hydrograph separation to improve understanding of dissolved organic carbon dynamics in headwater catchments. *Hydrol. Process.* **2014**, *28*, 5354–5366. [CrossRef]

39. Keene, W.C.; Galloway, J.N. Organic acidity in precipitation of North America. *Atmos. Environ. (1967)* **1984**, *18*, 2491–2497. [CrossRef]

40. Sedlak, D.L.; Hoigné, J. The role of copper and oxalate in the redox cycling of iron in atmospheric waters. *Atmos. Environ. Part A Gen. Top.* **1993**, *27*, 2173–2185. [CrossRef]